JFBE 2(2): 101-106, 2019

Journal of Food and Bioprocess Engineering

Journal homepage: https://jfabe.ut.ac.ir

Original research

Biodegradable kefiran-chitosan-nanocellulose blend film: Production and physical, barrier, mechanical, thermal, and structural properties

Hanie Salmanian, Faramarz Khodaiyan*, Seyed Saeid Hosseini

Bioprocessing and Biodetection Laboratory, Department of Food Science and Engineering, University of Tehran, Karaj - Iran - Postal Code 31587-77871

ABSTRACT

In this study, biodegradable kefiran-chitosan-nanocellulose blend films were developed and their physical, mechanical, barrier, thermal and structural properties determined. Results showed that adding nanocellulose had not any significant effect on the thickness, moisture content and water solubility. Also, water vapor permeability, tensile strength and lightness increased and the elongation at break, glass transition and melting temperatures, chromaticity parameters of red–green and yellow–blue, total color difference, and whiteness index decreased by increasing the nanocellulose content. Scanning electron microscopy demonstrated that at high concentrations of nanocellulose, the nanoparticle dispersion was not uniform and many agglomerations observed in the surface and cross-section of the nanocomposites. In the end, XRD analysis showed that the dispersed phase of nanocellulose could not indicate its own crystalline peaks in the kefiran-chitosan matrix.

Keywords: Nanocomposite, Mechanical properties, Thermal properties

Received 8 January 2019; Received 19 March 2019; Accepted 27 March 2019

1. Introduction

The plastics, as a product of fossil fuels, attributed to their large availability, low price, lightness, transparency and other suitable properties have been applied as packaging material in food industry for long time. However, this material due to their total non-biodegradability caused damage to environment (Sabaghi et al., 2015; Motedayen et al., 2013; Zehetmeyer et al., 2017). In recent years, due to these negative environmental impacts and also limited oil resources, the food industry has been encouraged to use the natural bio-based materials and polymers in packaging (Ghasemlou et al., 2011b; Wang & Jing, 2017). These edible and biodegradable materials are usually made from polysaccharides, proteins and lipids, alone and/or in combination together (Zolfi et al., 2014a; Alparslan, 2017). So far, the many studies on biopolymer-based packaging materials obtained from naturally renewable resources such as starch (Almasi et al., 2010), zein (Ghanbarzadeh et al., 2006), gluten (Gontard et al., 1994), kefiran (Ghasemlou et al., 2011) and chitosan (Ojagh et al., 2010) have been done.

Kefiran, as a water soluble exopolysaccharide produced by *Lactobacillus kefiranofaciens* subsp. *Kefiranofaciens* present in kefir grains, is a branched glucogalactan containing approximately equal amounts of glucose and galactose (Piermaria et al., 2011). This polysaccharide, which has antibacterial, antifungal and antitumor properties, often as a texturing and gelling agent in the food industry is applied (Piermaria et al., 2008; Cevikbas et al., 1994). Also, the results obtained from several studies showed that the kefiran can produce edible films with good appearance, physical and mechanical properties and therefore, it can has an excellent potential in production of these type of films (Ghasemlou et al., 2011).

Chitosan, as a heteropolysaccharide obtained from chitin by N-deacetylation, is isolated from crustacean shells such as crab and shrimp (Crouvisier-Urion et al., 2017; Bonilla & Sobral, 2016). So far, because of the excellent antioxidant and antibacterial properties and also good biodegradability of this polysaccharide, the many studies on its application in biosensors, tissue engineering, water treatment and edible films have been conducted (Yang et al., 2016; Chetouani et al., 2017).

However, the obtained edible films from these polysaccharides due to their hydrophilic nature have weaker the barrier and mechanical properties, compared with plastics material (Sabaghi et al., 2015; Wang & Jing, 2017). Therefore, these weaknesses of the films might be improved by different physical and chemical modifications including biopolymers blending, addition of plasticizing agents such as glycerol and nanofiller materials such as nanocellulose (Zolfi et al., 2014a; Qazanfarzadeh & Kadivar, 2016).

In recent years, the cellulose nanocrystals have gained particular attention as nanofiller material because of unique physical and chemical properties (Corsello et al., 2017). In addition

*Corresponding author.
E-mail address: Khodaiyan@ut.ac.ir (F. Khodaiyan).

to the unique properties such as low density and high biodegradability rate of these nanocrystals, they also are cheaper than other nanofillers using in production of nanocomposites (Dehnad et al., 2014). Therefore, the aim of this study was to investigate the effect of adding nanocellulose on the physical, barrier, mechanical, thermal, and structural properties of the biodegradable films obtained from mixing kefiran and chitozan biopolymers.

2. Material and Methods

2.1. Materials

Kefir grains were supplied from a household in Karaj, Iran. Chitosan and nanocellulose were obtained from Sigma Chemical Co. (St. Louis, MO, USA) and Nano Novin Polymer Co. (Mazandaran, Iran). Acetic acid, glycerol, calcium chloride, sodium chloride, magnesium nitrate, nutrient broth and Mueller-Hinton agar were purchased from Merck Chemical Co. (Darmstadt, Germany).

2.2. Preparation of films

First, the kefiran exopolysaccharides were extracted from kefir grains by the method of Piermaria et al. (2009), and then the nanocomposite films prepared by casting technique (Zolfi et al., 2014a; Bonilla & Sobral, 2016). For this purpose, the aqueous solution of 1 % w/v kefiran was prepared by weighing the amount of film-forming solution under stirring condition for 15 min. Also, chitosan solution (1 %w/v) was produced by adding 1g of chitosan into 100 mL of acetic acid under constant magnetic stirring for 12 h at 40°C. Then, glycerol (20 %w/w based on dry matter weight) was added as a plasticizer to both solutions and stirring continued for a further 15 min. In the next step, the film-forming solution was prepared by mixing ratio 70:30 (the best ratio determined by pre-tests) kefiran and chitosan solutions. In the following, due to removing the air bubbles incorporated during stirring, the film solutions were transferred into a vacuum oven for 30 min at 30°C. The cellulose nanocrystals were added very slowly to distilled water and dispersed by ultrasonication and then mixed with the film-forming solutions to prepare composites containing 0, 5, 10 and 15 wt% nanocellulose (dry weight). After the stirring for 1h, the film solutions were poured onto Teflon petri dishes and dried at room temperature and relative humidity (RH) for about 18 h. In the end, dried films were separated from plates and stored inside desiccators at 25 ± 1°C and 50% RH prior to the experimental analysis.

2.3. Evaluation of physical properties of films

2.3.1. Thickness

The films thickness was measured by a hand-held micrometer (Mitutoyo No. 293-766, Tokyo, Japan) with sensitivity of 0.001 mm. For each sample, the thickness of 10 random points was measured and the mean values applied in calculations related to permeability and mechanical tests.

2.3.2. Moisture content

The moisture content of films (approximately 1×3 cm^2) was measured by determining the weight loss of samples before and after drying in an oven (103 ± 2°C) until a constant weight was obtained.

2.3.3. Water solubility of films

The water solubility of films was assessed using the method described by Gontard et al. (1994) with a slight modification. This parameter, as the percentage of the water-soluble dry matter of each film that is dissolved after 24 h immersion in water, was calculated as follows:

$$\text{TSM}\ (\%) = \frac{W_1 - W_2}{W_1} \times 100 \qquad (1)$$

where TSM was the total soluble matter of films, W_1 was initial dry weight of films and W_2 was final dry weight of samples after immersed in 50 mL of distilled water (24 h, 25°C) and dried in oven (103 ± 2°C, until to reach constant weight).

2.4. Water vapor permeability (WVP)

The WVP of films was determined according to the standard method E96 (ASTM, 1995). The cups with wide rims and diameter, depth and volume of 12.62 mm, 43 mm and 10 mL, respectively, were used to evaluate of this parameter. The films with different concentration of nanocellulose and without pinholes or defects were sealed to the cup (contain approximately 50 g anhydrous calcium chloride desiccant (~ 0% RH, test cup) or nothing (control cup)) mouths by paraffin. Then, the films were placed in desiccators maintained at 75% RH atmosphere with a sodium chloride saturated solution. Driving force (water vapor partial pressure of 1753.55 Pa) corresponds to water vapor transmission from the desiccator to cup is due to this RH difference. After the films were mounted, the weight of whole assembly was recorded every 1 h during 24 h, and every cup was shaken horizontally after each weighing. In the end, to obtain the rate of water vapor transmission, the slope of the weight-versus-time plot was divided by film area and the WVP for each type of nanofilm was calculated as follows:

$$\text{WVP}\ (\text{g/m.s.Pa}) = \frac{\text{WVTR} \times \text{X}}{\Delta \text{P}} \qquad (2)$$

where WVTR was water vapor transmission rate ($g/m^2.s$), X was film thickness (m) and ΔP was the vapor partial pressure difference across the film (Pa).

2.5. Mechanical properties

The tensile strength (TS) and elongation at break (EB) according to ASTM standard method D882-02 (ASTM, 2001), by a Testometric Machine M350-10CT (Testometric Co., Ltd., Rochdale, Lancs., England) were determined. First, the films were cut in rectangular strips (10×100 mm^2) and then equilibrated at 51% RH for 48 h in a desiccator by saturated $Mg(NO_3)_2$ solution. Subsequently, the films were fixed with an initial grip separation of 50 mm and stretched at a cross-head speed of 50 mm/min. The TS and EB were calculated by Eqs. (3) and (4).

$$TS\ (Pa) = \frac{F_{max}}{A} \quad (3)$$

$$EB\ (\%) = \frac{L_2 - L_1}{L_1} \times 100 \quad (4)$$

where F_{max}, A, L_1 and L_2 were the maximum load (N), the initial cross-sectional area (m^2), the initial length of specimen (m) and the final length of specimen (m), respectively.

2.6. Determination of the thermal properties

Thermal properties of the nanocomposite films were studied by Differential Scanning Calorimetry (DSC) equipment (Mettler Toledo, DSC1 Star System). 10 mg sample was cut and placed into aluminum DSC pan (an empty aluminum pan was applied as reference). The film samples were heated by instrument under a nitrogen atmosphere at 20 mL/min velocity and heating rate of 10°C/min between temperatures ranging from –50 to 150°C. The glass transition temperatures (T_g) and melting peaks (T_m) were eventually determined on the basis of the midpoint temperature of a step-down shift in baseline (related to the discontinuity of the specific heat) and temperature where the peak of the endotherm occurs, respectively (Ghasemlou et al., 2011a).

2.7. Surface color measurement

In this section, the film surface color was evaluated by a colorimeter (Minolta CR 300 Series, Minolta Camera Co., Ltd., Osaka, Japan). The film samples were placed on a white standard plate (L^*= 93.49, a^*= –0.25 and b^*= –0.09) and then, L [lightness; between 0 (black) and 100 (white)] and chromaticity parameters a [red–green; between –80 (greenness) and 100 (redness)] and b [yellow–blue; between –80 (blueness) and 70 (yellowness)] were determined. Also, total color difference (ΔE) and whiteness index (WI) were calculated by Eqs. (5) and (6) (4m4).

$$\Delta E = \sqrt{(L^* - L)^2 + (a^* - a)^2 + (b^* - b)^2} \quad (5)$$

$$WI = 100 - \sqrt{(100 - L)^2 + a^2 + b^2} \quad (6)$$

where L^*, a^*, and b^* were the standard color parameter values and L, a, and b were the sample color parameter values.

2.8. Scanning electron microscopy (SEM)

The SEM (Oxford Instruments INCA Penta FET-X3) at accelerating voltage of 15 kV was used to observe the surface and cross-sections of the dried films with or without nanocellulose. After being broken in liquid nitrogen, the films mounted on aluminum stubs by a double-sided tape and then coated with a thin layer of gold in the ionizer of metals (BAL-TEC AG, Balzers, Liechtenstein).

2.9. X–ray diffraction (XRD) analysis

The XRD patterns of the nanofilms with the concentrations of 0, 5, 10 and 15% nanocellulose were analyzed by an X'Pert MPD diffractometer (Philips Co., Holland). The XRD patterns were recorded using Cu Kα radiation with wavelength of 1.542 Å and a nickel monochromator with voltage of 40 kV and current of 30 mA. The XRD patterns were obtained at room temperature with 2θ varying between 5° and 55° with a scanning rate of 1°/min.

2.10. Statistical analysis

The all experiments were conducted in triplicate using a completely randomized design. The analysis of variance (ANOVA) and Duncan's multiple ranges test were applied to compare the difference among mean values of treatments at the level of 0.05 by SPSS 13 (Version 11.5; SPSS Inc., Chicago, USA) software.

3. Results and Discussion

3.1. Physical properties of films

The results due to the thickness of nanoomposite films were showed in Table 1. As can be seen in this table, the thickness was ranged from about 0.037 to 0.039 mm. In addition, the value of the parameter for this nanofilm was lower than kefiran film reported by Ghasemlou et al. (2011b), which could be due to the presence of nanoparticles in very small size and also the difference in film-making procedures.

Observations related to the moisture content of nanofilms showed that this parameter was varied between 10.41 to 13.60% (Table 1). Also, the results showed that adding nanocellulose did not have significant effect on this parameter ($p < 0.05$).

Water solubility is an important property of biopolymer-based films, which is due to materials hydrophilicity of film and also the total empty volume occupied by water in network of film microstructure (Li et al., 2011; Ghasemlou et al., 2011). The water solubility values of the control films and nanofilms containing the different concentrations of cellulose nanoparticles were showed in Table 1. It can be seen that although water solubility was varied between about 17.49 to 21.88%, the results demonstrated that adding nanocellulose in different concentrations had not significant effect on this parameter ($p < 0.05$).

3.2. Water vapor permeability

The WVP, due to its relation with food spoilage, is one of the most important properties packaging films. The WVP of films was evaluated and the observations are shown in Table 1. The results demonstrated that the WVP values increased with an increase in cellulose nanoparticles content ($p < 0.05$). This increase in WVP value could be due to the aggregation and self-condensation of nanocellulose in different concentrations and therefore making empty spaces in composite matrix (Chaichi et al., 2017). These findings also are in line with many studies (Mandal & Chakrabarty, 2015; Reddy & Rhim, 2014).

3.3. Mechanical properties

The mechanical properties of kefiran-chitosan based nanocomposites containing different concentrations of cellulose nanoparticles were indicated in Table 1. As can be seen, the TS of nanocomposites increased from about 16.32 to 24.08 MPa with an increase in concentration of nanocellulose from 0 to 15%. This increase in TS and thereby mechanical properties of nanocomposites is probably duo to the inherent strength of cellulose nanoparticles related to the hydrogen bonds of intra- and

intermolecular and also the suitable interfacial interaction between nanocellulose and the kefiran-chitosan matrix (Qazanfarzadeh & Kadivar, 2016).

The investigation of the effect of nanocellulose on the EB properties showed that this parameter decreased significantly ($p < 0.05$) from 140.08 to 125.22% when nanocellulose content inccreased up to 15%. This achievement could be due to the rigid nature of cellulose nanoparticles and also limiting motion of the kefiran-chitosan matrix related to the strong interactions between the nanocellulose and this matrix (Bamdad et al., 2006). Additionally, this result was in accordance with result obtained from alginate-based nanocomposites containing nanocrystalline cellulose by Hug et al. (2012).

Table 1. Effect of various concentrations (5, 10 and 15%) of nanocellulose (N-Cel) on the thickness, moisture content (MC), water solubility (WS), water vapor permeability (WVP), tensile strength (TS), elongation at break (EB), glass transition temperatures (T_g), melting peaks (T_m), color values (*L*, *a*, and *b*), total color difference (ΔE) and whiteness index (*WI*) of kefiran (Kef)-chitosan (Chi) films[A,B].

Sample	Thickness (mm)	MC (%)	WS (%)	WVP ($\times 10^{-11}$g/m s Pa)
Kef-Chi	0.039 ± 0.074[a]	13.60 ± 1.50[a]	21.88 ± 0.74[a]	8.53 ± 0.57[a]
Kef-Chi-5% N-Cel	0.037 ± 0.067[a]	10.41 ± 4.22[a]	17.49 ± 3.87[a]	18.85 ± 1.31[c]
Kef-Chi-10% N-Cel	0.037 ± 0.082[a]	13.28 ± 7.38[a]	18.25 ± 0.70[a]	22.61 ± 1.75[d]
Kef-Chi-15% N-Cel	0.038 ± 0.074[a]	10.54 ± 5.02[a]	19.37 ± 1.10[a]	14.36 ± 0.47[b]

	TS (MPa)	EB (%)	Tg (°C)	Tm (°C)
Kef-Chi	16.32 ± 0.22[a]	140.08 ± 0.28[c]	-41.50 ± 0.32[b]	79.90 ± 0.13[c]
Kef-Chi-5% N-Cel	16.47 ± 0.60[a]	131.11 ± 0.33[b]	-41.32 ± 0.25[b]	77.78 ± 0.22[b]
Kef-Chi-10% N-Cel	20.12 ± 0.33[b]	130.42 ± 0.37[b]	-43.51 ± 0.14[a]	75.58 ± 0.14[a]
Kef-Chi-15% N-Cel	24.08 ± 0.13[c]	125.22 ± 0.18[a]	-43.33 ± 0.18[a]	75.35 ± 0.17[a]

	L	*a*	*b*	*ΔE*	*WI*
Kef-Chi	40.53 ± 1.88[a]	0.19 ± 0.16[a]	-0.04 ± 0.02[a]	13.54 ± 2.04[b]	40.53 ± 1.88[b]
Kef-Chi-5% N-Cel	46.44 ± 3.28[b]	0.25 ± 0.06[a]	-1.77 ± 0.02[c]	12.92 ± 3.26[b]	29.03 ± 0.33[a]
Kef-Chi-10% N-Cel	52.97 ± 1.99[c]	0.29 ± 0.08[a]	-1.67 ± 0.16[c]	6.49 ± 1.90[a]	28.83 ± 0.26[a]
Kef-Chi-15% N-Cel	53.26 ± 1.12[c]	0.18 ± 0.03[a]	-0.93 ± 0.15[b]	6.39 ± 1.11[a]	29.13 ± 0.10[a]

[A] Means within each column with same letters are not significantly different ($p < 0.05$).
[B] Data are means ± SD.

3.4. Thermal properties

The thermal properties of films are important to characterize their processing temperature limit and application. As can be seen, the T_g and T_m of nanocomposites are summarized in Table 1. The T_g, as a complex phenomenon, is related to different factors such as intermolecular interaction, flexibility of chain conformations and molecular weight of the material (Khoo et al., 2016). Table 1 demonstrated that the T_g of nanocomposites was shifted to low temperature with increasing the cellulose nanoparticles content from 0 to 15% (– 40.50 to – 43.33°C, respectively). These results are in line with results reported by Zolfi et al. (2014a), who studied the effect of TiO_2 on the kefiran-whey protein isolate based films. Also, the T_m decreased from 79.70 (0% cellulose nanoparticles) to 75.35°C (15% cellulose nanoparticles), which this observation was probably related to the regularity disruption of the structure of chains in kefiran-chitosan matrix and increasing the space between the biopolymer chains (Nakayama & Hayashi, 2007). In addition, this result agreed with Khoo et al. (2016)'s work who investigated the effect of nonacellulose on the poly (lactic acid) and reported the T_m of nanocomposites decreased with an increase in concentration of nanocellulose.

3.5. Color measurement

The color is another important property of nanocomposites in a product's acceptability to consumers. The parameters of *L*, *a*, *b*, ΔE and *WI* are present in Table 1. In general, the *L*- and *b*-values of nanocomposites were increased and decreased with increasing the cellulose nanoparticles, respectively, while adding the nanocellulose had not any significant effect on the *a*-value. The increase in *L*-value could be due to the hydrophilic property of nanocellulose and its compatibility with hydrophilic biopolymers of kefiran and chitosan (Zolfi et al., 2014b). Also, the decrease in *b*-value showed that the blueness and yellowness in nanocomposites has increased and decreased, respectively. In addition, the results indicated that the ΔE and *WI*, which indicate the degree of total color difference from the standard color plate and degree of whiteness factors, respectively, were decreased with an increase in concentration of cellulose nanoparticles of nanocomposites.

3.6. Scanning electron microscopy (SEM)

In this work, for study of microstructure of films, SEM was applied to describe the surface and cross-section topography of composites with different concentrations of cellulose nanoparticles (Fig. 1). As can be seen, the surface and cross-section morphology of the kefiran-chitosan film was smooth and homogenous, while adding nanocellulose leaded to a rough surface and decreased the homogeneity and smoothness of surface and cross-section of the nanocomposites films. Fig. 1 shows at low concentration (5%) of nanocellulose, the nanoparticles were approximately well distributed in kefiran-chitosan matrix. On the contrary, at high concentrations of this nanoparticle (10 and 15%), dispersion of nanocellulose was not uniform and many agglomerations observed in the surface and cross-section of the films. These results are probably related to form stacked particles, because the nanoparticles due to high interfacial area and surface energy could interact with each other and form this granular structure (Qazanfarzadeh & Kadivar, 2016). The results obtained from this part are similar to other nanofilms such as kefiran-whey protein-TiO_2 and alginate-nanocellulose films in the study of Zolfi et al. (2014b) and Abdollahi et al. (2013), respectively.

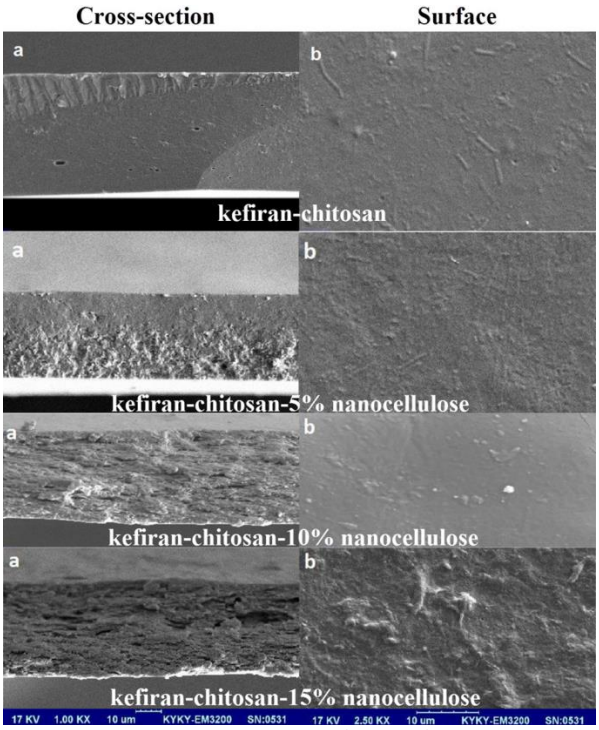

Fig. 1. Scanning electron micrographs of the surface (right) and cross-section (left) of kefiran-chitosan films containing different concentrations of nanocellulose.

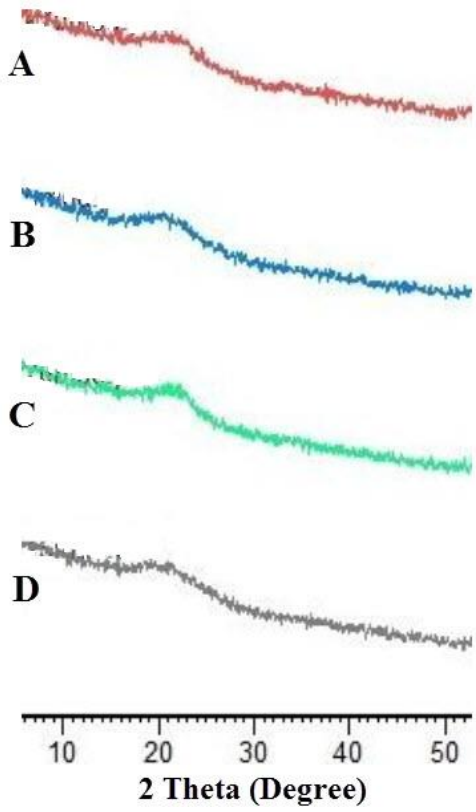

Fig. 2. XRD patterns for (A) kefiran-chitosan, (B) kefiran-chitosan-5% nanocellulose, (C) kefiran-chitosan-10% nanocellulose, and (D) kefiran-chitosan-15% nanocellulose.

3.7. X–ray diffraction (XRD)

The XRD patterns of the kefiran-chitosan film and kefiran-chitosan-nanocellulose composite films with different nanoparticle concentrations were showed in Fig. 2. According to this figure, the kefiran-chitosan and nanocomposite films demonstrated one broad peak at 2θ of about 22°. This broad peak showed an amorphous structure in the nanofilms. Fig. 2 shows that addition of nanocellulose into kefiran-chitosan film did not significantly change in the peak position. Therefore, it can be said that the dispersed phase of nanocellulose cannot show its own crystalline peaks in the kefiran-chitosan matrix, which this is due to predominately amorphous of kefiran-chitosan matrix and very low proportion of nanocellulose and thereby, overcome of the diffraction pattern of cellulose nanoparticles by kefiran-chitosan (Chaichi et al., 2017). Also, the similar results with this part were reported by several researchers (Mandal & Chakrabarty, 2015; Mathew & Dufresne, 2002).

4. Conclusion

Abstract The observations provided beneficial data about different properties of kefiran-chitosan-nanocellulose blend films. Increasing of the cellulose nanoparticles content had not significant effect on the physical properties such as thickness (~ 0.037 to 0.039 mm), moisture content (~ 10.41 to 13.60%) and water solubility (~ 17.49 to 21.88%), but increased water vapor permeability (~ 8.53 to 22.61×10^{-11} g/m s Pa) and tensile strength (~ 16.32 to 24.08 MPa), and decreased elongation at break (~ 125.22 to 140.08%) and thermal properties such as glass transition (~ – 41.32 to – 43.51°C) and melting (~ 75.35 to 79.90°C) temperatures. Also, the color measurement showed that blueness and yellowness in nanocomposites has increased and decreased, respectively. SEM micrographs demonstrated a uniform distribution for the nanocomposites containing 10 and 15% of nanocellulose. The XRD patterns showed that incorporation of nanoparticles had not significant effect on the kefiran-chitosan pattern.

References

Abdollahi, M., Alboofetileh, M., Behrooz, R., Rezaei, M., & Miraki, R. (2013). Reducing water sensitivity of alginate bio-nanocomposite film using cellulose nanoparticles. *International Journal of Biological Macromolecules, 54*, 166–173.

Almasi, H., Ghanbarzadeh, B., & Entezami, A. A. (2010). Physicochemical properties of starch–CMC–nanoclay biodegradable films. *International Journal of Biological Macromolecules*, *46*(1), 1–5.

Alparslan, Y. (2017). Antimicrobial and antioxidant capacity of biodegradable gelatin film forming solutions incorporated with different essential oils. *Journal of Food Measurement and Characterization*, 1–6.

ASTM (1995). *Standard test methods for water vapor transmission of material, E 96–95. Annual book of ASTM*. Philadelphia, PA: American Society for Testing and Material.

ASTM (2001). *Standard test method for tensile properties of thin plastic sheeting. Standard D882. Annual book of ASTM*. Philadelphia, PA: American Society for Testing and Materials.

Bamdad, F., Goli, A. H., & Kadivar, M. (2006). Preparation and characterization of proteinous film from lentil (*Lens culinaris*): Edible film from lentil (*Lens culinaris*). *Food Research International*, *39*(1), 106–111.

Bonilla, J., & Sobral, P. J. A. (2016). Investigation of the physicochemical, antimicrobial and antioxidant properties of gelatin-chitosan edible

film mixed with plant ethanolic extracts. *Food Bioscience*, *16*, 17–25.

Cevikbas, A., Yemni, E., Ezzedenn, F. W., Yardimici, T., Cevikbas, U., & Stohs, S. J. (1994). Antitumoural antibacterial and antifungal activities of kefir and kefir grain. *Phytotherapy Research*, *8*(2), 78–82.

Chaichi, M., Hashemi, M., Badii, F., & Mohammadi, A. (2017). Preparation and characterization of a novel bionanocomposite edible film based on pectin and crystalline nanocellulose. *Carbohydrate Polymers*, *157*, 167–175.

Chetouani, A., Follain, N., Marais, S., Rihouey, C., Elkolli, M., Bounekhel, M., … Le Cerf, D. (2017). Physicochemical properties and biological activities of novel blend films using oxidized pectin/chitosan. *International Journal of Biological Macromolecules*, *97*, 348–356.

Corsello, F. A., Bolla, P. A., Anbinder, P. S., Serradell, M. A., Amalvy, J. I., & Peruzzo, P. J. (2017). Morphology and properties of neutralized chitosan-cellulose nanocrystals biocomposite films. *Carbohydrate Polymers*, *156*, 452–459.

Crouvisier-Urion, K., Lagorce-Tachon, A., Lauquin, C., Winckler, P., Tongdeesoontorn, W., Domenek, S., … Karbowiak, T. (2017). Impact of the homogenization process on the structure and antioxidant properties of chitosan-lignin composite films. *Food Chemistry*.

Dehnad, D., Mirzaei, H., Emam-Djomeh, Z., Jafari, S.-M., & Dadashi, S. (2014). Thermal and antimicrobial properties of chitosan–nanocellulose films for extending shelf life of ground meat. *Carbohydrate Polymers*, *109*, 148–154.

Ghanbarzadeh, B., Oromiehie, A. R., Musavi, M., Razmi, E., & Milani, J. (2006). Effect of polyolic plasticizers on rheological and thermal properties of zein resins. *Iranian Polymer Journal*, *15*(10), 779.

Ghasemlou, M., Khodaiyan, F., & Oromiehie, A. (2011). Physical, mechanical, barrier, and thermal properties of polyol-plasticized biodegradable edible film made from kefiran. *Carbohydrate Polymers*, *84*(1), 477–483.

Ghasemlou, M., Khodaiyan, F., Oromiehie, A., & Yarmand, M. S. (2011a). Characterization of edible emulsified films with low affinity to water based on kefiran and oleic acid. *International Journal of Biological Macromolecules*, *49*(3), 378–384.

Ghasemlou, M., Khodaiyan, F., Oromiehie, A., & Yarmand, M. S. (2011b). Development and characterisation of a new biodegradable edible film made from kefiran, an exopolysaccharide obtained from kefir grains. *Food Chemistry*, *127*(4), 1496–1502.

Gontard, N., Duchez, C., Cuq, J., & Guilbert, S. (1994). Edible composite films of wheat gluten and lipids: water vapour permeability and other physical properties. *International Journal of Food Science & Technology*, *29*(1), 39–50.

Huq, T., Salmieri, S., Khan, A., Khan, R. A., Le Tien, C., Riedl, B., … Kamal, M. R. (2012). Nanocrystalline cellulose (NCC) reinforced alginate based biodegradable nanocomposite film. *Carbohydrate Polymers*, *90*(4), 1757–1763.

Khoo, R. Z., Ismail, H., & Chow, W. S. (2016). Thermal and morphological properties of poly (lactic acid)/nanocellulose nanocomposites. *Procedia Chemistry*, *19*, 788–794.

Li, Y., Jiang, Y., Liu, F., Ren, F., Zhao, G., & Leng, X. (2011). Fabrication and characterization of TiO 2/whey protein isolate nanocomposite film. *Food Hydrocolloids*, *25*(5), 1098–1104.

Mandal, A., & Chakrabarty, D. (2015). Characterization of nanocellulose reinforced semi-interpenetrating polymer network of poly (vinyl alcohol) & polyacrylamide composite films. *Carbohydrate Polymers*, *134*, 240–250.

Mathew, A. P., & Dufresne, A. (2002). Morphological investigation of nanocomposites from sorbitol plasticized starch and tunicin whiskers. *Biomacromolecules*, *3*(3), 609–617.

Motedayen, A. A., Khodaiyan, F., & Salehi, E. A. (2013). Development and characterisation of composite films made of kefiran and starch. *Food Chemistry*, *136*(3), 1231–1238.

Nakayama, N., & Hayashi, T. (2007). Preparation and characterization of poly (l-lactic acid)/TiO 2 nanoparticle nanocomposite films with high transparency and efficient photodegradability. *Polymer Degradation and Stability*, *92*(7), 1255–1264.

Ojagh, S. M., Rezaei, M., Razavi, S. H., & Hosseini, S. M. H. (2010). Development and evaluation of a novel biodegradable film made from chitosan and cinnamon essential oil with low affinity toward water. *Food Chemistry*, *122*(1), 161–166.

Piermaria, J. A., Mariano, L., & Abraham, A. G. (2008). Gelling properties of kefiran, a food-grade polysaccharide obtained from kefir grain. *Food Hydrocolloids*, *22*(8), 1520–1527.

Piermaria, J. A., Pinotti, A., Garcia, M. A., & Abraham, A. G. (2009). Films based on kefiran, an exopolysaccharide obtained from kefir grain: Development and characterization. *Food Hydrocolloids*, *23*(3), 684–690.

Piermaria, J., Bosch, A., Pinotti, A., Yantorno, O., Garcia, M. A., & Abraham, A. G. (2011). Kefiran films plasticized with sugars and polyols: water vapor barrier and mechanical properties in relation to their microstructure analyzed by ATR/FT-IR spectroscopy. *Food Hydrocolloids*, *25*(5), 1261–1269.

Qazanfarzadeh, Z., & Kadivar, M. (2016). Properties of whey protein isolate nanocomposite films reinforced with nanocellulose isolated from oat husk. *International Journal of Biological Macromolecules*, *91*, 1134–1140.

Reddy, J. P., & Rhim, J.-W. (2014). Characterization of bionanocomposite films prepared with agar and paper-mulberry pulp nanocellulose. *Carbohydrate Polymers*, *110*, 480–488.

Sabaghi, M., Maghsoudlou, Y., & Habibi, P. (2015). Enhancing structural properties and antioxidant activity of kefiran films by chitosan addition. *Food Structure*, *5*, 66–71.

Wang, S., & Jing, Y. (2017). Effects of formation and penetration properties of biodegradable montmorillonite/chitosan nanocomposite film on the barrier of package paper. *Applied Clay Science*, *138*, 74–80.

Yang, W., Owczarek, J. S., Fortunati, E., Kozanecki, M., Mazzaglia, A., Balestra, G. M., … Puglia, D. (2016). Antioxidant and antibacterial lignin nanoparticles in polyvinyl alcohol/chitosan films for active packaging. *Industrial Crops and Products*, *94*, 800–811.

Zehetmeyer, G., Meira, S. M. M., Scheibel, J. M., da Silva, C. de B., Rodembusch, F. S., Brandelli, A., & Soares, R. M. D. (2017). Biodegradable and antimicrobial films based on poly (butylene adipate-co-terephthalate) electrospun fibers. *Polymer Bulletin*, *74*(8), 3243–3268.

Zolfi, M., Khodaiyan, F., Mousavi, M., & Hashemi, M. (2014a). Development and characterization of the kefiran-whey protein isolate-TiO_2 nanocomposite films. *International Journal of Biological Macromolecules*, *65*, 340–5.

Zolfi, M., Khodaiyan, F., Mousavi, M., & Hashemi, M. (2014b). The improvement of characteristics of biodegradable films made from kefiran–whey protein by nanoparticle incorporation. *Carbohydrate Polymers*, *109*, 118–125.